The Behavior of Manganese in Oxygen Steelmaking

Rout B.[1], Brooks, G.[1], Rhamdhani, M. A.[1], Li, Z.[2] and van der Knoop, W.[3]

1 .Department of Mechanical and Product Design Engineering
Swinburne University of Technology,
John Street, Hawthorn, Melbourne, Victoria 3122 Australia
2. WMG, University of Warwick
Coventry CV4 7AL, UK
3. Tata Steel Technology, 1970CA Ijmuiden, The Netherlands
Email: gbrooks@swin.edu.au, Ph.: +61 3 9214 5672

Keywords: Manganese, Oxygen Steelmaking, Process Modelling

INTRODUCTION

Manganese serves as an important alloying element in commercial grades of steel and high levels of Mn can improve the mechanical properties of steel. [1] The chemical behavior of Mn in Oxygen Steelmaking is complex because the element is readily oxidised in conditions found in steelmaking but the stability of its oxide is a strong function of temperature and slag chemistry, and the oxide can readily revert back to elemental Mn in steelmaking conditions. In many steel plants, manganese ore has been added to achieve high Mn at the end blow. This approach means that the use of relatively expensive ferromanganese (FeMn) can be reduced in the subsequent secondary steelmaking process. [1] Steel plants can also face the problem of high Mn (>1 wt pct) in the hot metal due to the use of lean iron ores with high MnO in the blast furnace, and this can cause operational issues in the steelmaking process. [2]

The Mn refining profile commonly observed in basic oxygen furnace (BOF) shows a rapid oxidation at the beginning of the blow followed by back reduction of Mn from slag to metal during the middle stage of the blowing and finally some further oxidation later in the blow, as shown schematically in Figure 1. The oxidation reactions associated with this behavior can take place at the hot spot (where the jet impacts onto the bath) according to equation (1), at the bath-slag interface where (FeO) is the principal provider of oxygen for the reaction, according to equation (2) and at the slag/droplet interface(s) in the emulsion. The reversion reaction between carbon dissolved in iron and MnO, as per equation 3, can also be expected to place between droplets in the emulsion and slag, and at the interface between the bath and slag. Figure 2 shows schematically the major zones of the furnace where these reactions can be expected to take place.

$$[Mn] + \tfrac{1}{2}\, O_2(g) = (MnO) \quad (1)$$

$$(FeO) + [Mn] = (MnO) + [Fe] \quad (2)$$

$$[C] + (MnO) = [Mn] + CO(g) \quad (3)$$

Several researchers reported that the transfer of Mn between the liquid metal and slag is controlled by the oxygen potential, determined by Fe/Fe_tO equilibrium according to the reaction 2. [1, 3 and 6] Mass transfer equations have been formed to describe the kinetics of this reaction, assuming that equilibrium is reached at the interface.[1] In the case of the droplets in the emulsion, the mass transfer of Mn is expected to be driven by the generation of CO bubbles inside the droplets and mass transfer equations for this behavior has been developed by the authors to predict the extent of the reaction in droplets [11], though there is no experimental data for droplets currently available to validate these predictions, similar kinetics expressions for the removal of carbon, silicon and phosphorous have been validated against plant and experimental data. [11, 15-17]

The balance between the oxidation (equation 2) and reduction reaction (equation 3) in the droplets is complicated by limited knowledge of (a) the number and size of droplets in the emulsion at any one time, (b) the residence time of the droplets in the emulsion and the (c) the temperature of droplets in emulsion. Researchers at both McMaster University and Swinburne University of Technology have been addressing these issues over the last decade [12-18], through a combination of experimentation and modelling and they predicted that during the blow that there is a significant number of droplets in the emulsion in the size range of 1 to 5mm, spending between 20 to 50s in the emulsion during the first two thirds of the blow. The residence time of the droplets is controlled by the "bloating" of the droplets and this bloating is most pronounced when

the carbon level of the droplets is above 1 wt.%, at lower levels of carbon, the droplets are predicted to spend less than 1s in the emulsion.

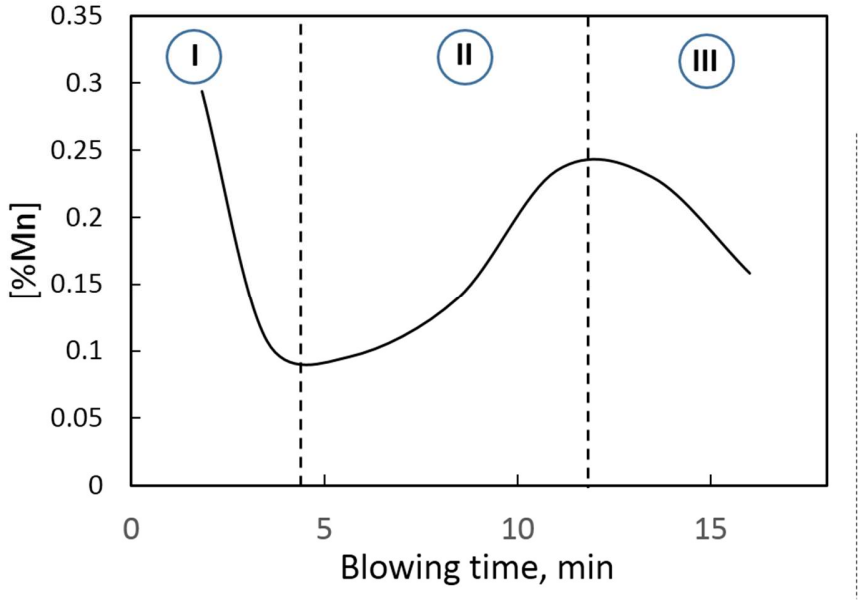

Figure 1: Typical manganese refining path in a top blowing converter. Region I: rapid manganese oxidation, Region II- manganese reversion from slag to metal, Region III: manganese oxidation [15)

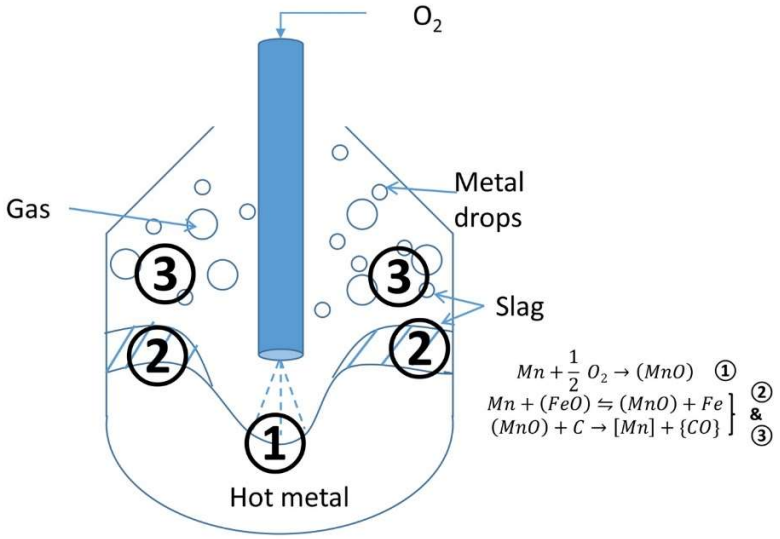

Figure 2: Schematic representation of oxidation/reduction reactions of Mn across various interfaces in a BOF [15]

Researchers at Swinburne University of Technology have been working with Tata Steel researchers on developing a multi-zone dynamic model of BOF steelmaking. [11, 13-15] A schematic diagram of the model's structure is shown in Figure 3. It is beyond the scope of this paper to fully describe the details of this model but key features include: (i) incorporation of the generation, residence time and reactions of droplets in the slag emulsion as a function of time, (ii) calculation of kinetics of de-C in the hot spot as function of lance position, (iii) inclusion of flux dissolution, (iv) including scrap melting/dissolution, and allows to predict how the concentration of different elements in different zones of the furnace vary with time. [11, 13-15]

The modelling does not involve curve fitting or introduction of fitting factors, instead where ever possible scientifically based formulae from either laboratory studies or fundamental theory has been used. The model does not include the heat transfer aspects of the process and rather enters in temperature profiles form measured plant data. The model has been validated using industrial data in the open literature [19, 20] and industrial data from the Tata works at IJmuiden. [21] In general the model predicts de-C and de-Si behaviour well, captures the general shape of the de-Mn and de-P curves. The model has revealed that the playoffs between FeO formation, de-C and post combustion of CO above the bath are critical to accurately capturing the kinetic details of the BOF process and that there is still a lack of understanding and data about this aspect of the process. These issues aside the model does provide a significant step forward in predicting the kinetic behavior of the BOF and the key results from the model relating to de-Mn are presented and discussed in this paper.

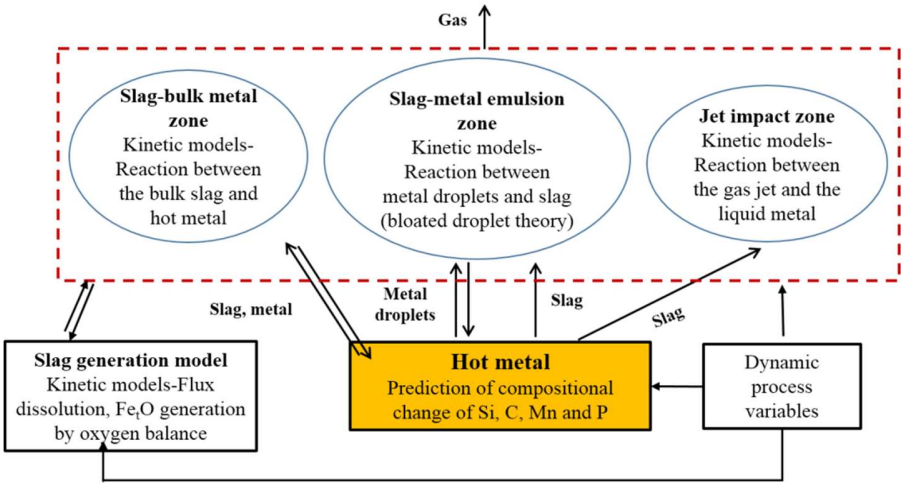

Figure 3: Schematic of multi-zone kinetic model for BOF process [21]

MULTI-ZONE MODEL OF MANGANESE KINETICS

The primary regions for Mn reaction in BOF have been illustrated in Figure 2. In this model the jet impact, slag- bulk metal and emulsion zones were considered to be the main zones for manganese refining. Full details of the model for de-Mn, shown schematically in Figure 3, are described in a journal paper recently submitted [15] with a summarized version provided below.

Mathematical modelling of overall Mn refining rate

The mathematical expression for the overall manganese refining rate can be written as:

The concentration of manganese in the bulk metal was calculated by the following mass balance equation:

$$W_b^{t+\Delta t} \times [\text{wt pct Mn}_b]^{t+\Delta t} = W_b^t \times [\text{wt pct Mn}_b]^t - \left(\frac{dW_{Mn}}{dt}\right)_{em} \times \Delta t - \left(\frac{dW_{Mn}}{dt}\right)_{iz} \times \Delta t - \left(\frac{dW_{Mn}}{dt}\right)_{sm} \times \Delta t + \left(\frac{dW_{Mn}}{dt}\right)_{sc} \times \Delta t \quad (4)$$

Here, $\left(\frac{dW_{Mn}}{dt}\right)_{em}$, $\left(\frac{dW_{Mn}}{dt}\right)_{iz}$ and $\left(\frac{dW_{Mn}}{dt}\right)_{sm}$ are the rates of Mn removed from the emulsion, jet impact and slag-bulk metal zones respectively (kg/s). Δt is the numerical time step, $W_b{}^t$ is the weight of the hot metal (kg) at time t, $W_b^{t+\Delta t}$ is the weight of the hot metal at next time step $(t + \Delta t)$, and [wt pct Mn_b] is the weight percentage of Mn in the bulk metal.

The change in mass of the bulk metal was estimated using the calculated mass of scrap, droplet generation and return to bath, slag and gas formation during time Δt, as per equation (5):

$$W_b^{t+\Delta t} = W_b^t - \Delta W_m^{sl,t} + \Delta W_{sc}^{m,t} - \left(\frac{dW_c}{dt}\right)_{em} \times \Delta t - \left(\frac{dW_c}{dt}\right)_{iz} \times \Delta t \quad (5)$$

Here $W_b^{t+\Delta t}$ is the weight of the bulk metal at time t + Δt, W_b^t is the weight of the bulk metal at time step t, $\Delta W_m^{sl,t}$ is the weight of the hot metal (Fe, Si, Mn and P) converting into slag and $\Delta W_{sc}^{m,t}$ is the weight of the melted scrap during time step Δt. $\left(\frac{dW_c}{dt}\right)_{em}$ and $\left(\frac{dW_c}{dt}\right)_{iz}$ is the rate of carbon (kg/s) removed through emulsion and jet impact zone respectively.

Modeling of Mn reaction kinetics at jet impact area

The rate of Mn oxidation at jet impact area, can be expressed as a first order rate law assuming the reaction to be controlled by mass transfer in the hot metal.

$$\left(\frac{\mathrm{dW_{Mn}}}{\mathrm{dt}}\right)_{\mathrm{iz}} = -\mathrm{k_m} \times \frac{\mathrm{A_{iz}}}{100} \times \rho_{\mathrm{m}}([\text{wt pct Mn}] - [\text{wt pct Mn}]_{\mathrm{iz}}^{\mathrm{eq}}) \quad (6)$$

Here k_m is the mass transfer coefficient, A_{iz} is the area of the jet impact and ρ_m is density of steel. The value of $[wt\ pct\ Mn]_{iz}^{eq}$ was estimated from the following equations:

$$[\mathrm{Mn}] + [\mathrm{O}] = (\mathrm{MnO}),\ \log K_{\mathrm{MnO}} = 12760/T - 5.62 \quad (7)$$

$$1/2\ O_2 = [\mathrm{O}],\ \log K_O = 6170/T + 0.125 \quad (8)$$

The overall equilibrium constant for the Mn oxidation reaction according to Eq. 1 is given by:

$$\log K = \log K_{\mathrm{MnO}} + \log K_o \quad (9)$$

In these calculations, the oxygen partial pressure, P_{O2} is assumed to be 1 atm (1.013×10^5 Pa) and activity of MnO, a_{MnO} has been calculated by regular solution model developed by Ban-Ya. [22] The measured thermal profile of hot spot reported by Chiba *et al*. [23] has been used to simulate the temperature in the jet impact area. A relationship proposed by Kitamura *et al*. [24] has been used to determine the mass transfer coefficient of Mn in the melt phase.

$$\log k_m = 1.98 + 0.5 \log\left(\frac{\varepsilon H^2}{100L}\right) - \frac{125000}{2.3RT} \quad (10)$$

where k_m is the mass transfer coefficient in metal phase (cm/s), ε is the stirring energy (W/t), H and L are the bath depth (cm) and diameter (cm) of the furnace respectively and T is the temperature in the impact zone (K). The total stirring energy was calculated by using the combined effect of the top and bottom gas injection in the BOF. [15]. A calculation of cavity area as a function of blow parameters was performed but the cavity coalescence was ignored and the overall cavity area was calculated by adding the individual cavity formed by each nozzle. [14]

Modelling of Mn reaction kinetics at slag-metal interface

The rate Mn transfer across the slag-bulk metal interface as a result of the reaction between [Mn] in the bulk metal and (FeO) in the slag is assumed to be controlled by the transport of both [Mn] in metal and (MnO), based on a previous study [25], using the following equation:

$$\left(\frac{dW_{Mn}}{dt}\right)_{sm} = -k_o^{sm} \times \frac{A_{sm}}{100} \times \rho_m \left\{[\text{wt pct Mn}] - \frac{(\text{wt pct Mn})}{L_{Mn}}\right\} \quad (11)$$

Where A_{sm} is the surface area at slag-bulk metal interface, k_o^{sm} is the overall mass transfer coefficient. k_m was caluclated from Eq. 10. The slag phase mass transfer coefficient was given by the following equation:[26]

$$k_s = a \exp\left(-\frac{37000}{RT}\right).\varepsilon^b \quad (12)$$

Where k_s is the mass transfer coefficient in slag phase (cm/s), R: gas constant ($J.mol^{-1}K^{-1}$), a and b are the empirical parameters, assumed to be 1.7 and 0.25 respectively. [26]

The manganese partitioning ratio at the interface between the slag and the metal can be defined as the ratio between the wt pct of Mn in slag to wt pct of Mn in the hot metal as:

$$L_{Mn} = \frac{(\text{wt pct Mn})^i}{[\text{wt pct Mn}]^i} \quad (13)$$

A model developed by Suito and co-workers was used to calculate the manganese equilibrium concentration. [4] The empirical correlation of k'_{Mn} proposed by Suito is as follows:

$$\begin{aligned}\log k'_{Mn} = -0.0180[&(\text{wt pct CaO}) + 0.23(\text{wt pct MgO}) + 0.28(\text{wt pct Fe}_t\text{O}) \\ &- 0.98(\text{wt pct SiO}_2) - 0.08(\text{wt pct P}_2\text{O}_5)] + \frac{7300}{T} - 2.697\end{aligned} \quad (14)$$

The apparent equilibrium constant k'_{Mn} is defined as:

$$k'_{Mn} = \frac{(\text{wt pct MnO})}{(\text{wt pct T.Fe}) \times [\text{wt pct Mn}]} \quad (15)$$

The interfacial area between slag and bulk metal (A_{sm}) was calculated by subtracting the cavity area resulted by top jet from the geometrical area of the bath surface.[15]

Modelling of Mn reaction kinetics in slag-metal emulsion

The reaction of Mn at metal drop-slag interface is considered to be controlled by the mass transfer of Mn inside the metal drop and MnO in the slag. Thus, a mixed controlled kinetic equation has been applied for evaluating the rate of reaction of metal droplets in the slag-metal emulsion. The rate of Mn removal by a single droplet can be expressed as:

$$\left.\frac{d[\text{wt pct Mn}]}{dt}\right|_{drop}^{em} = -\frac{A_{drop}}{V_{drop}} \times k_o^{em} \times \left\{[\text{wt pct Mn}] - \frac{(\text{wt pct Mn})}{L_{Mn}}\right\} \quad (16)$$

A_{drop} and V_{drop} are the area and volume associated with the single droplet in the emulsion and L_{Mn} is the equilibrium partition ratio of Mn between slag and metal droplet. The surface area of the droplet due to bloating behaviour has been estimated from the empirical correlation of density change of droplet as a function of decarburization rate and FeO wt pct in slag proposed by Brooks *et al.* [12] The mass transfer coefficient of Mn transport in the metal for a translating droplet was determined by employing surface renewal model as.

$$k_m^{drop} = 2 \times \sqrt{\frac{D_{Mn}}{\pi t_c}} = 2 \times \sqrt{\frac{D_{Mn} u}{\pi d}} \quad (17)$$

Here d and u are the droplet diameter (m) and velocity (m/s) respectively. D_{Mn} is the diffusion coefficient of Mn in molten metal (m^2/s). The temperature and viscosity effect on mass diffusivity was taken into account by applying the Stokes-Einstein

equation. [15] On the slag side, the mass transfer coefficient was calculated assuming the metal droplet to be a rigid sphere with a stream of slag surrounding it. [15] Models for droplet generation and the residence time of droplets in the emulsion developed by the authors [12, 13] were applied to this study, as described in [11, 15].

The following major assumptions have been made in developing the multi-zone kinetic model for demanganisation in a BOF process.

1. The mass transfer of manganese only takes place at three reactive zones i.e. (i) jet impact area, (ii) slag-bulk metal, and (iii) slag-metal-gas emulsion.
2. The manganese refining in the slag-metal emulsion and slag-metal bulk zone was assumed to be proceeded by Mn and FeO reaction.
3. The equilibrium manganese distribution ratio (L_{Mn}) between the metal drop and slag was assumed to be the same as between bulk metal and slag. Suito's empirical correlation of L_{Mn} was considered for the calculation of manganese equilibrium at metal drop-slag interface in the emulsion.
4. The size distribution measured in plant trials by Cicutti *et al.* were assumed to apply, with the initial droplet size spectrum assumed to vary between 2.3×10^{-4} m to 3.35×10^{-3} m.

The measured data from a 200 t combined blowing converter [19] and a 55 t top blowing BOF [20] were used for model validation. In both industrial trials samples of metal and slag are collected during seven different times of blowing from the start of the blow. In the kinetics analysis of manganese refining for Holappa's data [20], the measured dynamic slag data have been used as an input to the model calculation. For the model used for Cicutti's data [19], a dynamic slag generation model that includes the iron oxide rate model based on oxygen mass balance and a flux dissolution model have been incorporated. [11].

RESULTS and DISCUSSION

The major results from the modelling study are summarized in Figures 4, 5, 6 and 7. Figure 4 shows how different assumptions about the temperature of droplets effects the equilibrium predictions used in the kinetic models. When the temperature of the interface was maintained as the bulk metal temperature the equilibrium line was found to be always lower than the actual Mn in the metal. However, when the interface was raised to 100 °C and 200 °C, above the bulk temperature than equilibrium drive for reversion was predicted to occur earlier in the blow. Therefore, these results suggest that the temperature at the reaction interface is one of the significant factors that controls the oxidation and reduction behaviour of manganese in the top blowing process.

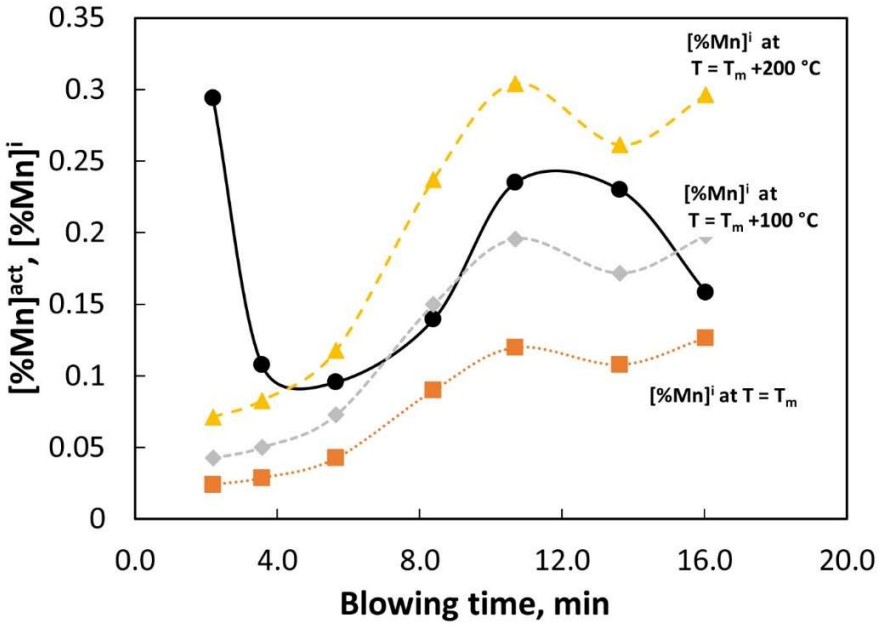

Figure 4: Effect of temperature on the equilibrium manganese at slag-metal interface (solid line- actual Mn in bath, dotted line- interfacial Mn concentration estimated at different slag-metal interface temperatures) [15]

The rate of manganese refined by the three distinct zones inside the BOF converter as a function of blowing time has been shown in Figure 5. In the jet impact region, the transfer of manganese from metal to slag was found to be increasing in the initial part of the blow for 200 t converter data reported by Cicutti *et al*. A decreasing trend has been observed for the 55 t converter operation during the initial stage. These differences in the Mn refining profile by jet impact zone during the starting period may be due to different lance practices used in the trials. The refining profile of Mn in jet impact area for the intermediate and final stage of converter operation were predicted to be similar for both the heats.

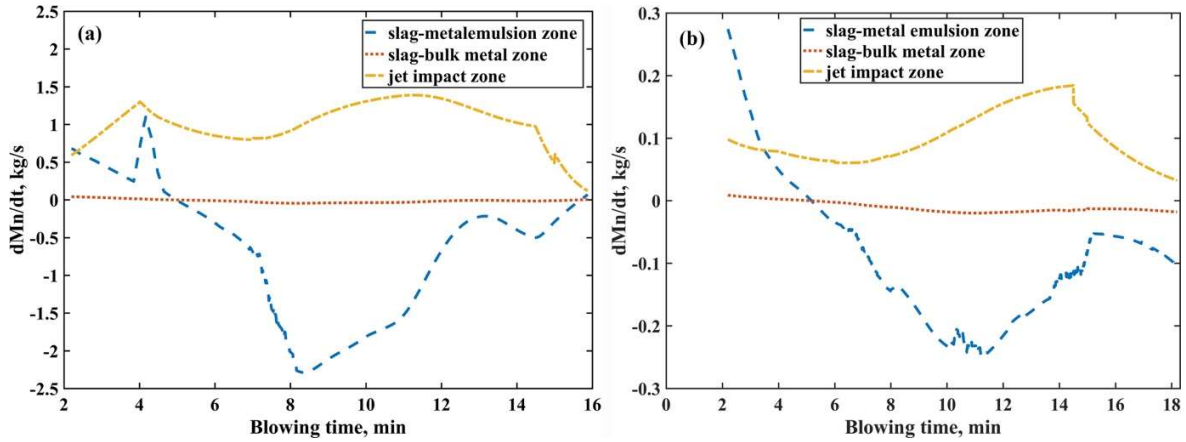

Figure 5: Mn removal rate calculated from different zones of the converter for (a) 200 t converter (b) 55 t converter [15]

The manganese removal rate by the circulating metal droplets in the emulsion has been computed for both industrial cases and shown in Figure 6. A significant fraction of manganese has been predicted to be transferred from slag to metal by the emulsion phase during the middle stage of the blow. Peak reversion rates were predicted to take place during 50 to 60% of blowing time. At the end stage of the blow the rate of manganese transfer by the droplets is very low. This is consistent with the general features of bloated droplet behaviour, as droplet residence times are expected to very low towards the end of the blow. [12] The rate of manganese transfer in the slag-bulk metal zone is predicted to be negligible as compared to jet impact and emulsion zone refining during the entire blow period, which is due to the very low interfacial area between the phases compared to the emulsion.

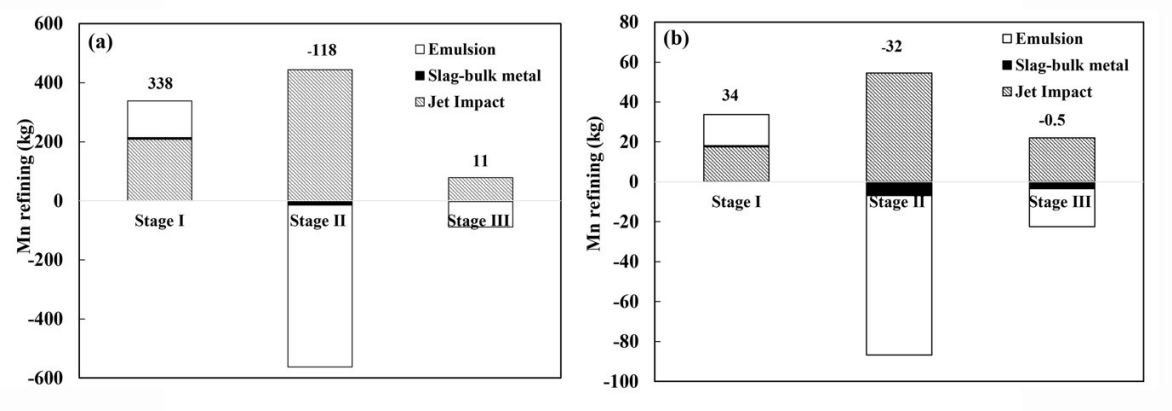

Figure 6: Total Mn exchange between metal and slag during stages of blow for (a) 200 t converter (b) 55 t converter for stages defined in Figure 1,[15]

The model prediction of change in concentration of Mn in the bulk metal as a function of blowing time is shown in Figure 7. The model calculation of Mn has been compared with the actual Mn value measured in the hot metal for two different converters. As can be seen, the predicted Mn profiles compare well with the actual Mn measurements from plant trials particularly during the early part of the blow. In the case of Cicutti's data, some deviation has been observed towards the end of the blow. It may be due to the inaccurate calculation of manganese equilibrium at slag-metal drop interface. Further experimental studies are needed to establish the manganese distribution between the slag and metal droplet in the emulsion.

Another possible explanation for the deviation is the sensitivity of the reversion predictions to the temperature at the slag droplet interface, where there is very limited data available. Certainly, the model provides a believable dynamic prediction of Mn behavior in the BOF, though further work is required to further develop key aspects of the model. For example, a heat transfer model could be developed to predict the surface temperature of the droplets in the emulsion and how this changes during the residence time of different droplets in the emulsion, which our model shows is an important parameter in predicting the reversion behavior during the blow. Also, no satisfactory model exist for predicting the kinetics of FeO formation in BOF steelmaking and this work we predict FeO through a mass balance approach. This does not allow us to understand how lance height and blowing parameters effect FeO formaton, which they obviously do.

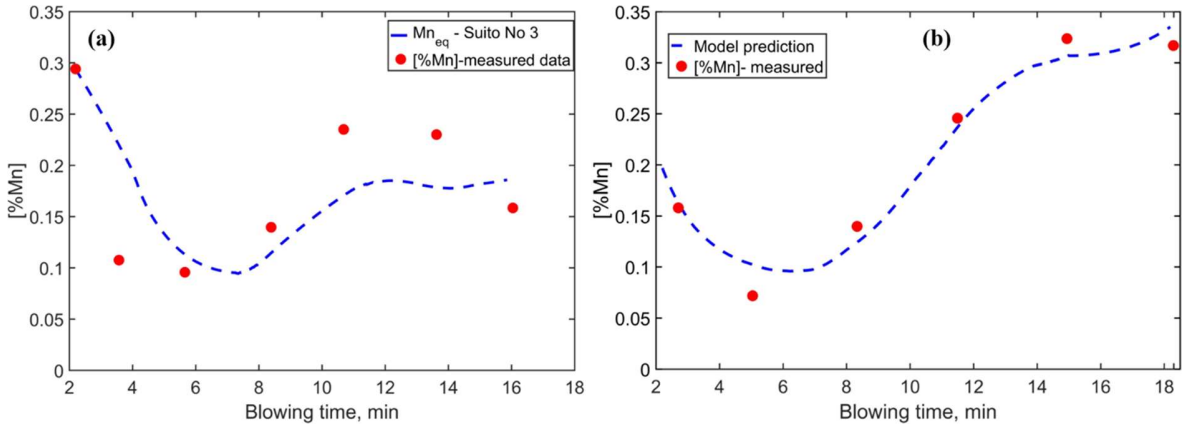

Figure 7: Model validation of Mn prediction in hot metal (a) Cicutti *et al.* data [19] (b) Hoppala *et al.* [20] data

CONCLUSIONS

A multi-zone kinetic model for Mn reaction in BOF has been developed and validated against industrial data. The computational model can predict the change in manganese concentration in the bulk metal during the blow period by estimating the rate of refining from different zones of the converter. The following conclusions are made from this study:

1. The model predicts that the temperature at the slag–metal drop interface plays a major role in deciding the oxidation and reduction nature of Mn reaction.
2. The kinetics of Mn refining in the first stage of the blow are predicted to be controlled by the oxidation of Mn by FeO in the emulsion and direct oxidation of Mn by O_2 in the jet impact zone.
3. The model predicts that the competition between the Mn oxidation in the jet impact zone and reduction of MnO by Fe by the metal droplets decides the direction of Mn transfer during middle and end period of the blow.
4. In the middle stage of the blow, after 30 to 40 % of blowing, a significant fraction of Mn reversion is predicted to take place in the emulsion zone
5. During the last stage of the blow, the refining of Mn is a result of simultaneous reaction at jet impact and emulsion zones.

The model developed provides believable predictions but further experimental and plant based work is required to verify key aspects of the chemical reactions being studies, such as temperature of the droplet interfaces during the blow and the equilibrium relationships between slag/metal over a wide range of conditions relevant to oxygen steelmaking.

ACKNOWLEDGEMENTS

The authors acknowledge their gratitude to Tata Steel for providing financial support for this work.

REFERENCES

1. A.T. Morales and R. J. Fruehan: *Metall. Mater. Trans. B*, 1997, vol. 28, pp. 1111-18.
2. D. Satish Kumar, R. Sah, V. R. Sekhar and S. C. Vishwanath: *Trans. Indian Inst.. Metals*, 2016, vol. 69, pp. 775-82.
3. H. Suito and R. Inoue: *ISIJ Int.* 1995, vol. 35, pp. 266-71.
4. H. Suito and R. Inoue: *Trans. of the Iron and Steel Institute of Japan*, 1984, vol. 24, pp. 257-65.

5. H. Suito and R. Inoue: *Trans. of the Iron and Steel Institute of Japan*, 1984, vol. 24, pp. 301-07.
6. C. Zhu, G. Li, Z. Chen, G. Ma and J. Liu: *ISIJ Int.,* 2008, vol. 48, pp. 123-29.
7. S. Jung: *ISIJ Int*. 2003, vol. 43, pp. 216-23.
8. W. L. Daines and R. D. Pehlke*: Metall. Trans.*, 1971, vol. 2, pp. 1203-11.
9. R. J. Pomfret and P. Grieveson: Ironmak. Steelmak., 1978, vol. 5, pp. 191-97.
10. T. Takaoka, I. Sumi, Y. Kikuchi and Y. Kawai: *ISIJ Int.,* 1993, vol. 33, pp. 98-103.
11. B. K Rout, G. Brooks, M. A. Rhamdhani, Z. Li, F.N. H. Schrama and J. Sun: *Metall. Mater. Trans. B,* 2018, vol. 1 pp 1-21
12. G. Brooks, Y. H. Pan, Subagyo and K. Coley: *Metall. Mater. Trans. B*, 2005, vol. 36, pp. 525-35.
13. B. K. Rout, G. A. Brooks, M. A. Rhamdhani and Z. Li: *Metall. Mater. Trans. B*, 2016, vol 47 (6), pp. 3350-61.
14. B.K Rout, G. Brooks, M. A. Rhamdhani, Z. Li, F. N. H. Schrama and A. Overbosch: *Metall. Mater. Trans. B*, 2017 (submitted).
15. B. K Rout, G. Brooks, M. A. Rhamdhani, Z. Li, F. N. H. Schrama and W. Van der Knoop: *Metall. Mater. Trans. B*, 2017. (submitted)
16. K. Gu, N. Dogan and K. Coley, *Metall. Mater. Trans. B,* 2017, vol. 48B, pp. 2343-2353
17. K. Gu, N. Dogan and K. Coley, *Metall. Mater. Trans. B,* 2017, vol. 48B, pp. 2595-2606
18. K. Gu, N. Dogan and K. Coley, *Metall. Mater. Trans. B*, 2017, vol. 48B, pp. 2984-3001
19. C. Cicutti, M. Valdez, T. Perez, J. Petroni, A. Gomez, R. Donayo, and L. Ferro *In Sixth International Conference on Molten Slags, Fluxes and Salts. Stockholm-Helsinki*, 2000.
20. L. Holappa and P. Kostamo*: Scand. J. Metallurgy,* 1974, vol. 3, pp. 56-60.
21. B. K. Rout , G.A. Brooks , Z. Li , M.A. Rhamdhani, Frank N. H. Schrama and A. Overbosch., *AISTech 2018*, AIST, Warredale, Pa.
22. S. Ban-Ya: *ISIJ Int.,* 1993, vol. 33, pp. 2-11.
23. K. Chiba, A. Ono, M. Saeki, M. Yamauchi, M. Kanamoto and T. Ohno: *Ironmak. Steelmak.,* 1993, vol. 20, pp. 215-20.
24. S. Kitamura, T. Kitamura, K. Shibata, Y. Mizukami, S. Mukawa and J. Nakagawa: *ISIJ Int.* 1991, vol. 31, pp. 1322-28.
25. Y. Kawai, N. Shinozaki, and K. Mori: *Canadian Metallurgical Quarterly, 1982,* vol. 21.4, pp. 385-91.
26. Y. Ogasawara, Y. Miki, Y. Uchida and N. Kikuchi: *ISIJ int*., 2013, vol. 53, no. 10, pp. 1786-1793